

Article

Detection of southern beech heavy flowering using Sentinel-2 imagery

Ben Jolly¹*, John R. Dymond¹, James D. Shepherd¹, Terry Greene², and Jan Schindler¹

¹ Manaaki Whenua – Landcare Research;

² Department of Conservation, New Zealand;

* Correspondence: jollyb@landcareresearch.co.nz

Version March 18, 2022 submitted to Remote Sens.

Abstract: The southern beech (*Fuscospora* and *Lophozonia*) forest in New Zealand periodically has 'mast' years where very large volumes of seed are produced. This excessive seed production results in a population explosion of rodents and mustelids that puts pressure on native birds. To protect the birds, extra pest control, costing in the order of 20 million dollars, is required in masting areas. To plan pest control and keep it cost-effective, it would be helpful to have a map of the masting areas. In this paper, we develop a remote sensing method for making a national map of beech flowering. It uses a temporal sequence of Sentinel-2 satellite imagery to determine areas where a yellow index based on red and green reflectance (red-green)/(red + green) is higher than normal in spring. The method was used to produce national maps of heavy beech flowering for the years 2017 through to 2021. In 2018, which was a major beech masting year, of the 4.1 million ha of beech forest in New Zealand, 27.6% was observed to flower heavily. The accuracy of the "heavy flowering detected" class was 90.4% and the accuracy of the "heavy flowering not detected" class was 91%. The method is fully automated and can be used to predict excessive seedfall, for all New Zealand, several months in advance of when pest control is required.

Keywords: southern beech; masting; beech flowering; seedfall; *Fuscospora*; Sentinel-2

1. Introduction

New Zealand southern beech (genus *Fuscospora* and *Lophozonia*, formerly *Nothofagus* [1]) forest dominates over 2 million hectares (ha) of New Zealand forest, and features in almost 2 million ha more [2]. It comprises five species: mountain beech (*Fuscospora cliffortioides*), red beech (*Fuscospora fusca*), silver beech (*Lophozonia menziesii*), black beech (*Fuscospora solandri*), and hard beech (*Fuscospora truncata*). These trees reproduce almost yearly, with periodic highly productive seasons known as 'mast' years that produce large volumes of seed [3]. Seed is a significant food source for a number of birds and mammals. Rodents and mustelids are of particular concern [4] because during mast years the rodent population increases significantly [4,5], providing an abundant food source for mustelids (esp. stoats – *Mustela erminea*) [6]. All rodent and mustelid species are non-native and prey on New Zealand native bird species, so increases in their populations are concerning. This compounds when the seed begins to run out and alternative food sources are sought as populations become unsustainable. Population control of introduced predators is essential for preserving native and endemic species of birds in New Zealand, especially in beech mast years [6].

The New Zealand Department of Conservation (DOC) is responsible for managing forests on public land, as well as preserving native species and coordinating pest control. They need to know when and where significant mast events occur for targeting pest control efforts to limit the explosion of predator populations [4]. A number of approaches are currently used for targeting: (i) modelling, (ii) field observations, and (iii) sampling of tree branches. (i) The 'delta-T' (ΔT) model [7] uses

35 the difference in mean temperature from the previous two summers ($T_{n-1} - T_{n-2}$) to predict likely
36 seedfall for the following autumn. This has been used to predict high seed yields at national scale.
37 However, it relies on temperature data, which are currently only available on a modelled 5 x 5 km
38 grid, so will miss smaller-scale micro-climate effects. While historical temperature is an important
39 factor in synchronizing mast events [7], other factors such as nutrient availability also play a role
40 [8]. New research suggests that rising temperatures due to climate change may change the masting
41 cycle of beech trees [8,9], increasing the spatial and temporal complexity of masting patterns [8] and
42 potentially desynchronizing flowering/seeding, effectively reducing the impact, and predictive power,
43 of temperature on the timing of the reproductive cycle [10]. (ii) Field staff from DOC are well-placed to
44 provide observations of beech flowering in certain areas as part of their normal duties. However, there
45 are large areas of forest that remain unobserved and spatial extent is often difficult to define, especially
46 at a regional or national scale. (iii) Finally, extensive sampling campaigns are conducted during years
47 where a heavy mast is expected using helicopters to clip upper branches from trees so seeds can be
48 counted. This task is expensive, labour-intensive, and dangerous.

49 Remote sensing has proved to be an effective tool for monitoring vegetation phenology,
50 particularly when a rich time series of imagery is available [11]. With sensors like Sentinel-2 it is
51 possible to map phenology over millions of hectares to create national maps at detailed scale (10m
52 pixels). Phenological characteristics are usually derived by first fitting a curve to the time series of
53 remote sensing data, then using either threshold-based methods, moving averages, inflection point,
54 or time of maximum increase [12]. Seasonality is usually assumed [12]. Vegetation indices such as
55 the normalised difference vegetation index (NDVI), the enhanced vegetation index (EVI), and the
56 normalised difference yellow index (NDYI), are often used to differentiate flowers and to summarise
57 data as one variable for analysis [12,13].

58 In this study, we investigate satellite remote sensing for identifying areas of significant southern
59 beech flowering in New Zealand. We use imagery from the European Space Agency (ESA) Sentinel-2
60 'a' and 'b' satellites to obtain a high rate of repeat passes to maximise the chances of multiple cloud-free
61 observations, and to produce national coverage at detailed scale. As significant flowering is an unusual
62 phenological event, we identify departures of NDYI from a normal annual pattern to identify heavy
63 beech flowering. Using this method, we produce national maps of heavy beech flowering for 5 different
64 years, 2017 through 2021. We assess the accuracy of the method by comparison with a human operator
65 at 1000 randomly selected sites. A national map of heavy beech flowering can be produced at the end
66 of every spring to assist DOC in identifying potential masting 'hot-spots' and thus aid planning of
67 pest control operations.

68 2. Materials and Methods

69 2.1. Data

70 The Sentinel-2 satellite mission consists of two satellites - Sentinel-2a and -2b - in sun-synchronous
71 orbits repeating every 10 days. These orbits are 180° out-of-phase with each other, which produces a
72 5-day revisit period. The swath width of each pass is 290 km, with five 'passes' required to cover the
73 mainland of New Zealand, each on a different day. Overlap between passes means that some areas
74 of the country have a higher revisit rate. Each Sentinel-2 satellite is equipped with a multi-spectral
75 imaging sensor capturing wavelengths from ultraviolet to short-wave infrared.

76 This study uses the Copernicus Sentinel-2 Level-1C calibrated top of atmosphere (TOA) reflectance
77 at the sensor as downloaded from the ESA archives, with edges masked to remove pixels that do not
78 contain data for every band. It covers all available Sentinel-2 data over New Zealand from 2016-09-01
79 to 2021-12-31, with images every 10 days before Sentinel-2b came online around 2017-07-08 and images
80 every 5 days thereafter. Analysis was restricted to areas of indigenous beech forest assumed as defined
81 by EcoSat Forests [2,14–16]. A 'mega-mast' occurred during spring 2018/autumn 2019 [17,18]. Other

82 years showed some small flowering events or none at all. Cloudy pixels were excluded from the
 83 temporal sequence using the methodology outlined in [19].

84 No suitable ground data on beech flowering exist to provide a reference dataset for accuracy
 85 assessment, however seed counts from a long-running monitoring programme using permanent seed
 86 traps [4] were available and supplied by DOC.

87 2.2. Methods

88 Southern beech flowers produce a reddening of the forest canopy that is easily visible from the
 89 ground, especially during a significant mast season. At the 10 m pixel nominal spatial resolution of
 90 Sentinel-2, the reddening of the canopy appears to the human eye as a subtle yellowing in the 'natural
 91 color' (RGB) image as the red flowers increase the red component of a pixel but not to the point of
 92 dominating the green. Higher-wavelength image bands (and associated indices) were investigated
 93 but the only other band that showed a noticeable response was Band 5 (red edge), and this was also
 94 associated with 'flushes' of new foliage in late spring. In order to detect the yellowing associated
 95 with southern beech flowering, we apply two approaches: the calculation of a normalised difference
 96 yellowing index (NDYI) to describe the red/green band relationship; and the modelling of this index
 97 over the time-series of the image archive to detect variations from the expected (non-flowering) state.

98 The effect is subtle enough that the technique required is very sensitive to cloud and shadow
 99 contamination. Additional to the cloud masking performed above, 'invalid' pixels from the cloud mask
 100 (cloud/shadow/snow/water) were buffered by 30 pixels (300 m) and patches of 'valid' pixels smaller
 101 than 100 ha were re-classified 'invalid'. Extra spectral filtering was then used to mask remaining
 102 pixels too bright or dark to be forest (or useful): $B4_{red} < 650$, $B3_{green} < 900$, $B2_{blue} < 1000$, $B8_{NIR} > 1000$,
 103 $B4_{red} - B5_{rededge} < -1500$. The result was then further buffered by 3 pixels.

104 The NDYI is similar to the well-known normalised difference vegetation index (NDVI)[20], using
 105 the 'red' (Band 4 665 +/- 15 nm) and 'green' (Band 3 560 +/- 18 nm) Sentinel-2 bands instead of
 106 'near-infrared' and 'red'. It is also very similar to the green-red vegetation index (GRVI)[21,22], with
 107 the order of the bands merely reversed:

$$108 \quad NDYI = \frac{(B4_{red} - B3_{green})}{(B4_{red} + B3_{green})} \quad (1)$$

109 The NDYI is calculated using the Level-1C TOA reflectance product re-projected to the New
 110 Zealand Transverse Mercator (NZTM) coordinate reference system (EPSG:2193) and with invalid pixels
 111 masked. As the NDYI represents the ratio of red-green, and both are affected similarly by transient
 112 atmospheric conditions, it will be negative over most areas of forest most of the time (i.e. when a pixel
 113 is 'green'), increasing to near or slightly above 0 during heavy flowering events. NDYI was calculated
 114 for cloud-free pixels mapped as beech in EcoSat Forests [2,14–16].

115 Substantial annual variation is present in TOA reflectance observations over forest due to climatic
 116 conditions, vegetation phenology, and sun angle. The NDYI signal visually observed during flowering
 117 is subtle enough in the context of a year of data that setting simple thresholds is inadequate to produce a
 118 reliable result. Additionally, flowering can occur at different times during the spring season, depending
 119 on latitude and altitude [3,8]. The temporal sequence of NDYI for a pixel in the Hawdon Valley (South
 120 Island, New Zealand) is shown in Figure 1 as an example. Part of the TMASK methodology developed
 121 for cloud detection in Landsat 8 imagery [23] was adapted to model the yellowing index for each pixel
 122 in areas of suspected beech forest (orange line in Fig. 1). The model uses robust regression to calculate
 123 coefficients for sine and cosine terms for intra- (a_1, a_2) and inter-annual (a_3, a_4) variability as well as
 124 a constant term (c) where x is the number of days since the start of the temporal sequence, T_{yr} is the
 125 number of days per year, and T_{all} is the number of days in the sequence:

$$126 \quad NDYI_{mod} = c + a_1 \sin\left(2\pi \frac{x}{T_{yr}}\right) + a_2 \cos\left(2\pi \frac{x}{T_{yr}}\right) + a_3 \sin\left(2\pi \frac{x}{T_{all}}\right) + a_4 \cos\left(2\pi \frac{x}{T_{all}}\right) \quad (2)$$

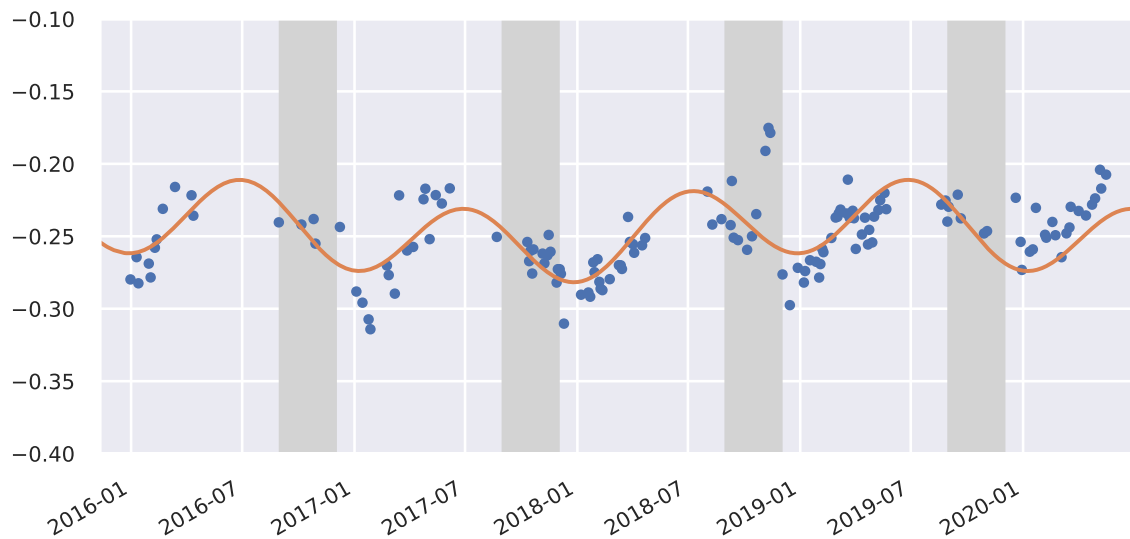


Figure 1. Observed NDYI values for an example pixel in the Hawdon Valley (blue) with modelled values (orange) superimposed. Grey areas indicate Spring seasons where NDYI is expected to peak during a mast.

125 Observed NDYI for each pixel/date were then subtracted from the modelled value to produce
 126 ΔNDYI and the maximum value was found for each flowering season (1st September to 10th
 127 December):

$$\Delta\text{NDYI} = \text{NDYI} - \text{NDYI}_{mod} \quad (3)$$

128 Finally, ΔNDYI values were converted to a map of 'heavy flowering detected' vs 'heavy flowering
 129 not detected' by following a method similar to Shepherd *et al.* [24]. First, a high ΔNDYI threshold of
 130 0.08 was chosen by assessing ΔNDYI against the seed trap data during the 2018 'mega mast'. This
 131 threshold was used to create 'seed' areas which were grown outwards by progressively lowering it
 132 to 0.04. The resulting 'flowering' pixels were then buffered by 2 pixels followed by a 5 × 5 majority
 133 filter then eroded by 2 pixels. 'Heavy flowering not detected' patches smaller than 1 ha were removed
 134 by re-coding as 'heavy flowering detected' or 'no data' (majority of surrounding pixels), then 'heavy
 135 flowering detected' patches smaller than 1 ha were re-coded 'heavy flowering not detected'.

136 As no ground truth data on flowering exist, the resulting national-scale map for the 2018 mast
 137 year was accuracy-assessed by a human operator. At 1000 randomly selected sites, 500 in "heavy
 138 flowering detected" and 500 in "heavy flowering not detected", the operator determined whether heavy
 139 flowering was observed in 2018 cloud-free spring imagery in comparison with a median spring image
 140 (excluding 2018).

141 3. Results

142 Spring (September/October/November) of 2017 was a light flowering season for southern beech
 143 in New Zealand. This was followed by a 'mega mast' in 2018 with heavy flowering observed from the
 144 ground during spring, and corresponding heavy seedfall the following autumn. Maps of maximum
 145 spring ΔNDYI were produced for each year of data, with results for the 2018 season shown in Figure
 146 2. Spatial patterns correspond with anecdotal reports from DOC staff based at field offices around
 147 New Zealand. There is heavy flowering throughout most of the north-western corner of the South
 148 Island, and sporadic heavy flowering in eastern Fiordland. The inset of Figure 2 highlights the level of
 149 detail available and shows heavy flowering on the lower slopes of the Hawdon and Poulter Valleys,

150 dissipating as altitude increases up the valley walls (black areas are not beech forest - either alpine or
 151 riverbed in this location).

152 Figure 3 shows the maps of heavy beech flowering as detected by the method for years 2017
 153 through 2021. In spring 2018, much heavy beech flowering was detected in the north-west of the South
 154 Island, synonymous with a 'mega mast' in that region. In the North Island and the south-west of the
 155 South Island, some pockets of heavy flowering were detected. The following year in spring 2019 the
 156 flowering was much reduced in the north-west of the South Island, but in the North Island much
 157 heavy flowering was detected, synonymous with another "mega mast". The south-west of the South
 158 Island had pockets of heavy flowering, much the same as in 2018. In years 2020 and 2021, minimal
 159 beech flowering was detected in most areas.

160 In the 2018 map, heavy flowering was detected in 27.6% of the 4.1 million ha of beech forest in
 161 New Zealand. Heavy flowering was not detected in 51.2% of the beech forest. In the remainder of the
 162 beech forest there was no cloud-free imagery in spring to make a decision. We assessed the accuracy of
 163 the 2018 map for heavy beech flowering. In each of the two classes, "heavy flowering detected" and
 164 "heavy flowering not detected", we generated 500 random locations at which we compared reference
 165 data with map data. Reference data was determined from visual interpretation of all the cloud-free
 166 spring imagery for the year. The "heavy flowering detected" class was 90.4% accurate and the "heavy
 167 flowering not detected" class was 91.0% accurate (Table 1 shows the confusion matrix).

Table 1. Confusion matrix of 2018 heavy flowering map. Proportions are estimated from a random sample of 500 locations in "Heavy flowering detected" class and a random sample of 500 locations in "Heavy flowering not detected" class.

		Reference classes			Proportion of mapped class	Map Accuracy
		Heavy flowering detected	Heavy flowering not detected	No cloud-free imagery		
Mapped classes	Heavy flowering detected	0.250	0.026	0.000	0.276	0.904
	Heavy flowering not detected	0.046	0.466	0.000	0.512	0.910
	No cloud-free imagery	0.000	0.000	1.000	0.212	1.000

168 4. Discussion

169 We developed a method that produces a national map of heavy beech flowering from a temporal
 170 sequence of Copernicus Sentinel-2 imagery (Fig. 3). The method detects elevated values of a yellow
 171 index, NDYI, above those normally expected in spring – a Δ NDYI value greater than 0.08 indicates
 172 heavy flowering. The elevated yellow index is caused by the production of red flowers obscuring
 173 green leaves. The national map of beech flowering may be produced at the end of spring, several
 174 months before the subsequent masting event actually occurs and seed drops to the ground. This gives
 175 the national agency in charge of pest control, DOC, several months to analyse the spatial distribution
 176 and intensity of the flowering in order to plan the extra pest control required. In the 2018 spring,
 177 a nationwide beech masting event was detected and mapped by this method. A manual accuracy
 178 assessment determined the method to be 90% accurate against a human operator with the same
 179 imagery. The spatial distribution of beech flowering as mapped by the method was also consistent
 180 with anecdotal observations from DOC field staff.

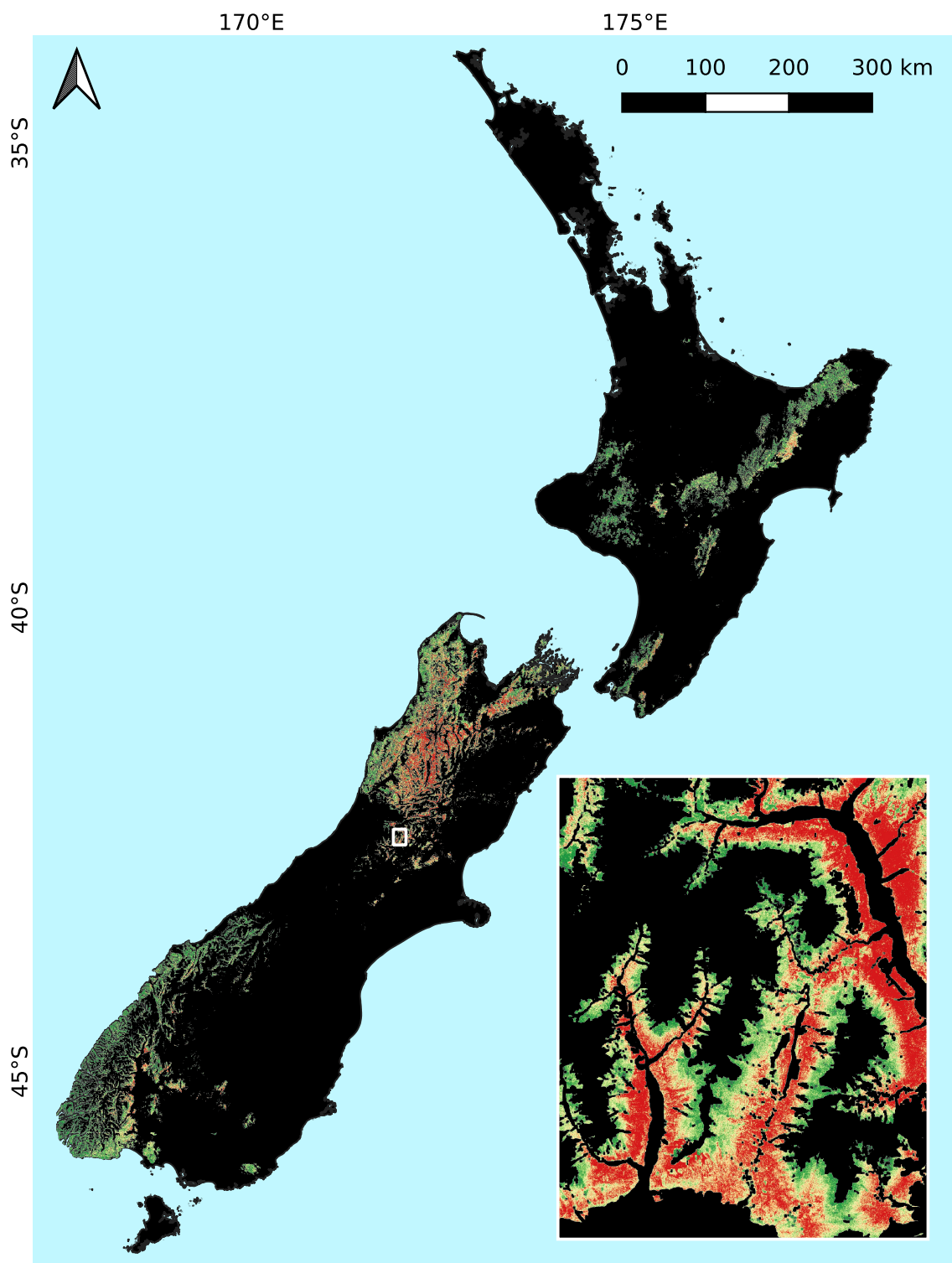


Figure 2. Maximum Δ NDVI (from modelled) for spring 2018 in areas of known southern beech forest in New Zealand. Green denotes areas of low (< 200) maximum Δ NDVI, while red is high (> 0.08) and indicates heavy beech flowering. Inset shows Hawdon and Poulter Valleys near Arthur's Pass (1:250,000 at 42.95°S, 171.82°E, see white box).

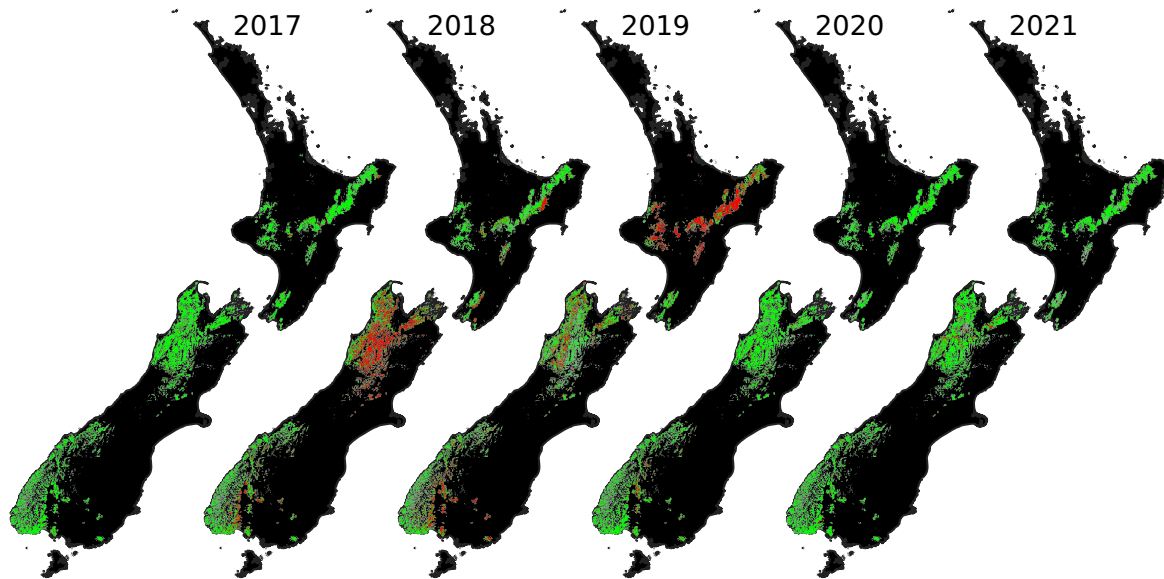


Figure 3. Maps of heavy beech flowering during spring time for four years of Sentinel-2 imagery (2017–2021 inclusive). Classes are "heavy flowering detected" (red), "heavy flowering not detected" (green), and "no cloud-free imagery" (grey).

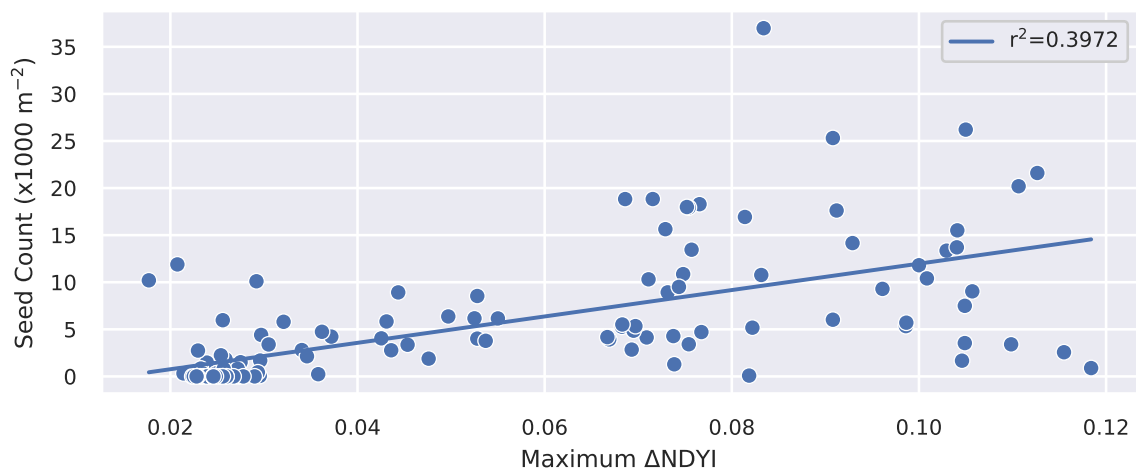


Figure 4. Relationship between maximum ΔNDVI (spring 2018) and number of seeds collected from seed traps in the permanent trap network (autumn/winter 2019) for the 2018/19 mast season. Locations are filtered to exclude those with fewer than eight valid satellite observations.

181 The national map of beech flowering can be used to provide extra detail to augment the existing
182 ΔT model, as it provides a higher spatial resolution of 10 m as opposed to 5 km. Observations of
183 flowering also help mitigate sources of uncertainty in the previous summer ΔT that could limit seed
184 production, such as carbon availability and soil moisture conditions [25]. The observations should also
185 mitigate the impact of microclimatic effects not captured in the modelled 5 km temperature grid. In
186 addition to the planning of extra pest control at appropriate scales, the national map of beech flowering
187 can be used for targeting observation/measurement campaigns investigating seedfall.

188 Not all heavy beech flowering in spring will result in heavy seedfall in the following autumn.
189 Heavy frost or very wet weather can interfere with seed production [3]. Figure 4 shows how well the
190 maximum Δ NDYI compares with seed counts in trays located on the floor of beech forest (seed
191 traps are spread throughout beech forests in New Zealand as part of long-running monitoring
192 programme conducted by DOC [4]). Data were restricted to locations with at least eight cloud-free
193 observations to obtain a fair representation over the majority of the spring season. There is noise in the
194 data, nevertheless high seed counts generally correspond with high maximum Δ NDYI. Reasons for
195 mismatches include: cloud coverage obscuring the flowering event (low Δ NDYI vs high seed count);
196 exact trap location relative to flowering trees as well as wind direction during seed fall (high Δ NDYI
197 vs low seed count); different beech species (different relationship between Δ NDYI and seed count);
198 climate, adverse weather events, and nutrient availability (lower seed count vs higher Δ NDYI); and
199 inaccuracies in the method (addressed in accuracy assessment). A similar comparison with 2017 data
200 (not shown) showed no relationship, seed counts were all 0 (or close to) and Δ NDYI values were very
201 low. We recommend the national map of flowering/not flowering be regarded as a map of potentially
202 high seedfall, to be confirmed later with additional information such as selected field observations.

203 In some areas there is a paucity of satellite observations – even with 5 daily or better repeats,
204 many mountainous areas of the country only receive a handful of cloud-free observations at irregular
205 intervals for an entire spring. The effect of this is that some areas of masting are missed as the
206 observations may not occur at times when the flowers are visible. A way to address this shortcoming is
207 to add more data sources. As the technique developed in this study relies only on red, green, blue, and
208 NIR (for quality control) wavelengths, it should be possible to include data from commercial satellite
209 constellations with higher revisit rates but lower spectral range or resolution, such as the Planet¹ 'Dove'
210 constellation. Targeted aerial imaging campaigns could also provide valuable information in areas of
211 known data paucity, particularly if they were informed by observations from field staff. This study has
212 shown the resolution requirement is low by aerial imaging standards which would allow higher flight
213 altitudes and larger image footprints, substantially reducing cost. Adding freely available Landsat-8
214 data could also increase the probability of obtaining a valid observation at a critical time.

215 Temporal analysis of Sentinel-2 satellite imagery has proved successful at detecting heavy
216 flowering in New Zealand beech forests. To achieve this, cloud clearing had to be accurate (because
217 the yellow index is sensitive to missed cloud) and automated (because many images are required).
218 Automation of the could clearing [19] and other processing means that beech flowering maps can be
219 produced in a timely and cost-effective way. In future, we plan to produce a national map of heavy
220 beech flowering at the end of each spring. This would give several months for analysis to plan the
221 extra pest control required in autumn, improving the targeting of pest control in masting areas, and
222 leading to better outcomes for native birds.

223 5. Conclusions

224 This study used Sentinel-2 top-of-atmosphere (TOA) imagery to detect and map atypical yellowing
225 associated with heavy flowering of southern beech (*Fuscospora* and *Lophozonia*) in New Zealand
226 over 4.1 million ha at an unprecedented 10 m spatial resolution. This was achieved by modelling

¹ <https://www.planet.com/>

227 a normalised difference yellowing index (NDYI) over 5 years of observations and investigating
228 deviations from expected values during spring months (September–November). A ‘threshold’ Δ NDYI
229 value of 0.08 may be used to identify areas of heavy flowering, with connected areas of Δ NDYI >
230 0.04 also likely flowering. The method has been automated and can be run for all of New Zealand in
231 less than a day on a cluster of approximately 1000 CPU cores. Using Sentinel-2 imagery, the method
232 typically provides information on heavy flowering for 80% of the beech forests in New Zealand with a
233 high accuracy of over 90%, producing helpful information for national-scale pest control efforts.

234 **Author Contributions:** Conceptualization, Ben Jolly, John Dymond, Terry Greene, and Jan Schindler; Data
235 curation, Ben Jolly, James Shepherd and Jan Schindler; Formal analysis, Ben Jolly; Funding acquisition, John
236 Dymond; Investigation, Ben Jolly, John Dymond, and Terry Greene; Methodology, Ben Jolly, John Dymond, James
237 Shepherd, and Terry Greene; Project administration, John Dymond; Resources, John Dymond; Software, Ben Jolly,
238 James Shepherd and Jan Schindler; Supervision, John Dymond; Visualization, Ben Jolly; Writing – original draft,
239 Ben Jolly; Writing – review & editing, John Dymond, James Shepherd, and Terry Greene.

240 **Funding:** This research was funded by the New Zealand Ministry of Business, Innovation and Employment
241 (MBIE) Endeavour Fund under the Advanced Remote Sensing of Aotearoa research programme (C09X1709).

242 **Acknowledgments:** The authors would like to thank the New Zealand Department of Conservation (DOC) for
243 providing advice and validation data.

244 **Conflicts of Interest:** The authors declare no conflict of interest. The funders had no role in the design of the
245 study; in the collection, analyses, or interpretation of data; in the writing of the manuscript, or in the decision to
246 publish the results.

247 Abbreviations

248 The following abbreviations are used in this manuscript:

249	DOC	Department of Conservation
	ESA	European Space Agency
	EVI	Enhanced vegetation index
	GRVI	Green-red vegetation index
250	NDVI	Normalised difference vegetation index
	NDYI	Normalised difference yellowing index
	NZTM	New Zealand Transverse Mercator
	TOA	Top of atmosphere

251

- 252 1. Heenan, P.B.; Smissen, R.D. Revised circumscription of Nothofagus and recognition of the segregate
253 genera Fuscospora, Lophozonia, and Trisyngyne (Nothofagaceae). *Phytotaxa* **2013**, *146*, 1–31.
254 doi:10.11646/phytotaxa.146.1.1.
- 255 2. Shepherd, J.D.; Ausseil, A.G.; Dymond, J.R. *EcoSat Forests: a 1: 750,000 scale map of indigenous forest classes
256 in New Zealand*; Manaaki Whenua Press, 2005.
- 257 3. Wardle, J.A. *The New Zealand beeches. Ecology, utilisation and management*; New Zealand Forest Service:
258 Wellington, New Zealand, 1984; p. 477.
- 259 4. Elliott, G.; Kemp, J. Large-scale pest control in New Zealand beech forests. *Ecological Management and
260 Restoration* **2016**, *17*, 200–209. doi:10.1111/emr.12227.
- 261 5. Ruscoe, W.A.; Pech, R.P. Rodent Outbreaks: Ecology and Impacts. In *Rodent outbreaks: ecology and impacts*;
262 Singleton, G.; Belmain, S.; Brown, P.; Hardy, B., Eds.; International Rice Research Institute: Los Baños
263 (Philippines), 2010; pp. 239–251.
- 264 6. King, C.M.; Powell, R.A. Managing an invasive predator pre-adapted to a pulsed resource: A model of
265 stoat (*Mustela erminea*) irruptions in New Zealand beech forests. *Biological Invasions* **2011**, *13*, 3039–3055.
266 doi:10.1007/s10530-011-9993-y.
- 267 7. Kelly, D.; Geldenhuis, A.; James, A.; Penelope Holland, E.; Plank, M.J.; Brockie, R.E.; Cowan, P.E.; Harper,
268 G.A.; Lee, W.G.; Maitland, M.J.; Mark, A.F.; Mills, J.A.; Wilson, P.R.; Byrom, A.E. Of mast and mean:
269 Differential-temperature cue makes mast seeding insensitive to climate change. *Ecology Letters* **2013**,
270 *16*, 90–98. doi:10.1111/ele.12020.

- 271 8. Allen, R.B.; Hurst, J.M.; Portier, J.; Richardson, S.J. Elevation-dependent responses of tree mast seeding to
272 climate change over 45 years. *Ecology and Evolution* **2014**, *4*, 3525–3537. doi:10.1002/ece3.1210.
- 273 9. Bogdziewicz, M.; Kelly, D.; Thomas, P.A.; Lageard, J.G.; Hackett-Pain, A. Climate warming
274 disrupts mast seeding and its fitness benefits in European beech. *Nature Plants* **2020**, *6*, 88–94.
275 doi:10.1038/s41477-020-0592-8.
- 276 10. Bogdziewicz, M.; Hackett-Pain, A.; Kelly, D.; Thomas, P.A.; Lageard, J.; Tanentzap, A.J. Climate warming
277 causes mast seeding to break down by reducing sensitivity to weather cues. *Global Change Biology* **2021**, p.
278 gcb.15560. doi:10.1111/gcb.15560.
- 279 11. Zeng, L.; Wardlow, B.D.; Xiang, D.; Hu, S.; Li, D. Remote Sensing of Environment A review of vegetation
280 phenological metrics extraction using time-series, multispectral satellite data. *Remote Sensing of Environment*
281 **2020**, *237*, 111511. doi:10.1016/j.rse.2019.111511.
- 282 12. Noumonvi, K.D.; Oblišar, G.; Žust, A.; Vilhar, U. Empirical approach for modelling tree phenology in
283 mixed forests using remote sensing. *Remote Sensing* **2021**, *13*. doi:10.3390/rs13153015.
- 284 13. Dixon, D.J.; Callow, J.N.; Duncan, J.M.; Setterfield, S.A.; Pauli, N. Satellite prediction of forest flowering
285 phenology. *Remote Sensing of Environment* **2021**, *255*, 112197. doi:10.1016/j.rse.2020.112197.
- 286 14. Dymond, J.R.; Shepherd, J.D. The spatial distribution of indigenous forest and its composition in the
287 Wellington region, New Zealand, from ETM+ satellite imagery. *Remote Sensing of Environment* **2004**,
288 *90*, 116–125. doi:10.1016/j.rse.2003.11.013.
- 289 15. Landcare Research Ltd. EcoSat Forests (North Island), 2014. doi:10.26060/STZ2-Z482.
- 290 16. Landcare Research Ltd. EcoSat Forest (South Island), 2014. doi:10.26060/2EPD-WE90.
- 291 17. Department of Conservation. Flowering and fruit production, 2019.
- 292 18. Department of Conservation. Department of Conservation Te Papa Atawhai Annual Report 2019. Technical
293 report, Department of Conservation, 2019.
- 294 19. Shepherd, J.D.; Schindler, J.; Dymond, J.R. Automated Mosaicking of Sentinel-2 Satellite Imagery. *Remote
295 Sensing* **2020**, *12*, 3680. doi:10.3390/rs12223680.
- 296 20. Rouse, W.; Haas, H.; Deering, W. Monitoring vegetation systems in the Great Plains with ERTS. NASA.
297 Goddard Space Flight Center 3d ERTS-1 Symposium, 1974.
- 298 21. Tucker, C.J. Red and Photographic Infrared I, Linear Combinations for Monitoring Vegetation. *Remote
299 Sensing of Environment* **1979**, *8*, 127–150. doi:10.1016/0034-4257(79)90013-0.
- 300 22. Motohka, T.; Nasahara, K.N.; Oguma, H.; Tsuchida, S. Applicability of Green-Red Vegetation Index for
301 remote sensing of vegetation phenology. *Remote Sensing* **2010**, *2*, 2369–2387. doi:10.3390/rs2102369.
- 302 23. Zhu, Z.; Woodcock, C.E. Automated cloud, cloud shadow, and snow detection in multitemporal Landsat
303 data: An algorithm designed specifically for monitoring land cover change. *Remote Sensing of Environment*
304 **2014**, *152*, 217–234. doi:10.1016/j.rse.2014.06.012.
- 305 24. Shepherd, J.D.; Dymond, J.R.; Cuff, J.R. Monitoring scrub weed change in the Canterbury region using
306 satellite imagery. *New Zealand Plant Protection* **2007**, *60*, 137–140. doi:10.30843/nzpp.2007.60.4671.
- 307 25. Uscoe, W.E.A.R.; Latt, K.E.H.P.; Richardson, S.J.; Allen, R.B.; Whitehead, D.; Carswell, F.E.; Ruscoe,
308 W.A.; Platt, K.H. Climate and net carbon availability determine temporal patterns of seed production by
309 Nothofagus. *Ecology* **2005**, *86*, 972–981.

310 © 2022 by the authors. Submitted to *Remote Sens.* for possible open access publication
311 under the terms and conditions of the Creative Commons Attribution (CC BY) license
312 (<http://creativecommons.org/licenses/by/4.0/>).